Title
The Influence Of Close-following Upon Cooling Module Air Flow

Authors
Browand, Fred
Marcu, Bogdan
Sharpe, Christian

Publication Date
1998

CALIFORNIA PATH PROGRAM
INSTITUTE OF TRANSPORTATION STUDIES
UNIVERSITY OF CALIFORNIA, BERKELEY

The Influence of Close-Following Upon Cooling Module Air Flow

Fred Browand, Bogdan Marcu, Christian Sharpe
University of Southern California

California PATH Research Report
UCB-ITS-PRR-98-6

This work was performed as part of the California PATH Program of the University of California, in cooperation with the State of California Business, Transportation, and Housing Agency, Department of Transportation; and the United States Department of Transportation, Federal Highway Administration.

Report for MOU 245

February 1998

ISSN 1055-1425

The Influence of Close-Following Upon Cooling Module Air Flow (MOU 245)

by
Fred Browand
Bogdan Marcu
Christian Sharpe

Department of Aerospace Engineering
University of Southern California
Los Angeles, California 90089-1191

Work supported by
California Department of Transportation
and
PATH, University of California, Berkeley

Executive Summary

The purpose of this report is to experimentally determine the air flow through the cooling module (air-conditioning condenser plus engine radiator) of a Ford Windstar minivan when the van is operated at a fraction of a vehicle length behind a lead van. Pressures and temperatures are measured across the cooling module while the vans are in operation, and a standard calibration relates the pressure drop to the flow velocity through the cooling module. The Windstars are connected in tandem and driven on a test track at spacings of 0.22, 0.28, 0.38, 0.62, 0.88, and 1.0, expressed as fractions of the Windstar length. For the purposes of the test, an override switch is installed to allow the close-following van to be operated either with both cooling fans remaining on or with both fans disabled. Air flow is expressed either as a volume flow, in cubic meters per second, or as the fraction of the flow for a van operating in isolation at the same forward speed. With both fans disabled, the air flow is approximately twenty per cent of the isolation value at the shortest spacing, and increases to about sixty per cent at a spacing of one vehicle length. With both fans operating, the air flow is approximately fifty per cent of the isolation value at the shortest separation, and increases to about seventy per cent at one vehicle length separation. These represent substantial decreases in air flow, and will result in a diminished operating envelope for the vehicle in close-following.

I. Benefits and Concerns for Close-Following

Close-following is a strategy for relieving the congestion on urban highways. The concept imagines vehicles to be equipped with automatic braking, throttle and steering capability—as well as the necessary speed and position sensors, computers and communications hardware—to allow high speed travel (60-80 MPH, say) at spacings of much less than one car length. Only a fraction of vehicles can be expected to possess the necessary equipment, and these vehicles would probably operate in a dedicated lane. (Perhaps the present carpool lane would eventually serve such a purpose.) The potential benefit of close-following is great, and is discussed in several articles contained in the recent publication Automated Highway Systems, (Plenum Publishing, 1997). Briefly, it can be noted that maximum flow, or throughput, on a typical freeway occurs at vehicle spacings of approximately 35 meters. This 35 meter spacing for maximum throughput seems to be typical of many freeways, and has not diminished appreciably over the past twenty years in spite of the great improvements in automobile performance. Since a typical vehicle is about 5 meters in length, six or seven vehicles could be placed within this 35 meter gap. If the space were entirely eliminated by close-following, an increase in throughput by a factor of 6 or 7 would result. More careful estimates, which include the braking distances for accident avoidance between members within a platoon and between separate platoons, suggest that a more realistic throughput improvement would be a factor of between 2 and 3—which is nonetheless an immense increase (Kanaris, Ioannou & Ho 1997).

Additional benefits arise as a result of fuel savings from the orderly flow of traffic, and from the decrease in the drag of vehicles traveling in close proximity. These are two separate effects. The latter saving was documented in a series of wind tunnel tests which predicted that an eight-vehicle platoon would have an average drag coefficient of approximately half the value associated with a single vehicle in isolation. Moreover, all of the vehicles in the platoon participate in the drag savings including the lead vehicle (cf., Browand, Zabat & Tokumaru 1997). This surprising and counterintuitive result has recently been supported by full scale field tests conducted to measure the drag of each vehicle in a two-vehicle platoon (Hong, Marcu, Browand & Tucker 1998). Drag reduction can be expected to result in an approximately 25 per cent fuel saving per vehicle mile traveled.

Many difficulties must be overcome before such a concept can be put into practice. Obvious considerations are the establishment of necessary infrastructure, and the establishment of appropriate collision avoidance measures. Ultimately, close-following travel must be deemed sufficiently safe and reliable by the general public.

Lesser but still important technical issues include the quantity of air flow to the engine compartment, and the quantity and quality of air flow to the passenger compartment of a platooning vehicle. Another issue involves the visibility of passengers and operators of trailing vehicles under rain or snow conditions, or when there may be water or road debris present which can be lifted from the roadbed into the platoon flowfield

Air flow in-to and out-of the gap regions between closely spaced vehicles is necessarily restricted. We know from our recent field test experience that the gap flows are highly unsteady in time. Gaps involve complex flow separations from the forward vehicle, and flow reattachments to the trailing vehicle. These flowfields cannot be reliably estimated by computer simulation—even utilizing the most powerful computers available today. Furthermore, it will be years before such simulations become practical.

The present report addresses the question of cooling module air flow for the case of two close-following vehicles. The vehicles are Ford Windstar vans. One van is the gift of **Ford Motor Company**, and contains our own instrumentation. The second vehicle is an identical rental van (from Hertz). In operation, the rental van is employed as the forward or tow vehicle. Flexible cables of fixed length are secured between the two vehicles by means of detachable fittings which bolt to the underside of both vans. Gap lengths range from 0.22 car lengths to 1.0 car lengths. Cooling flow is also measured for the single van in isolation, to determine the most important ratio: *(flow during close-following)/(flow in isolation).*

The tests are performed at the **Honda Proving Center of California**, located twenty miles east of Mojave, California. The three-lane test track is approximately seven miles in circumference, and allows uninterrupted travel at our test speeds of 50, 60 and 70 mph.

The remainder of the report is organized into two chapters. The first of these describes the test procedures and the conditions of the test in considerable detail. The last chapter contains the results and a discussion of the results. Those readers who are not interested in the details of the experimental procedures may wish to skip the intermediate material and proceed directly to the third chapter.

The raw data, the Matlab programming used to reduce the data, and the Labview data acquisition programs are too extensive to be included as appendices. However, upon request, this information can be made available on a CD-ROM.÷

II. Procedures for Estimating Radiator Air Flow

1. How cooling flow measurements are normally performed

An automobile radiator is an obstruction to the air flow. There must be a greater pressure in front of the radiator than behind to provide the motive force for the flow. It is this pressure difference across the radiator core which characterizes the flow, and which can be utilized to determine the velocity of the air flow. We will refer to the pressure difference as the radiator static pressure drop or simply the radiator pressure drop. It is relatively difficult to measure pressure at the front and back of the radiator, but relatively easy to measure a related quantity, termed stagnation pressure. By definition, stagnation pressure is:

$$p_o = p + (1/2)*\rho*(U)^2 \qquad (1)$$

where p is the local pressure, ρ is the local air density and U is the local air velocity. Subtracting the stagnation pressure in front of the radiator from that behind (station 1 minus station 2) gives the following expression:

$$\Delta p = p_{o1} - p_{o2} = p_1 - p_2 + (1/2)*\rho_1*(U_1)^2 - (1/2)*\rho_2*(U_2)^2 \qquad (2)$$

For a constant air density ($\rho_1=\rho_2$), continuity of flow through the radiator requires $U_1=U_2$. Thus the difference in local stagnation pressure is exactly equal to the difference in local pressure—the desired quantity.

Stagnation pressure is measured by means of small Kiel probes placed at many points in front-of and behind the radiator. A close-up of a Kiel probe is shown in figure 1.

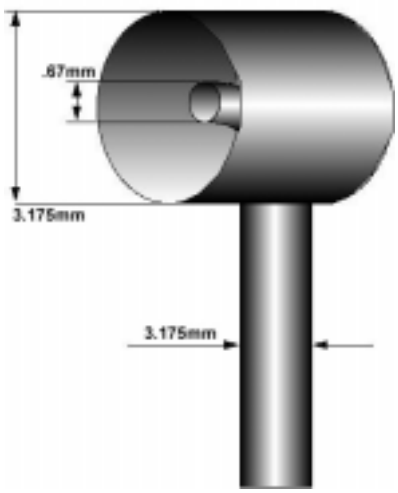

Figure 1. Kiel probes used in radiator pressure measurement.

The advantage of the Kiel probe geometry is that it is insensitive to the direction of the air velocity within a range of perhaps 60 degrees from the axis of the probe. The actual velocity vectors can be expected to lie within this range most of the time.

There exists a unique relationship between pressure drop and local flow velocity which is often expressed in the following form:

$$\Delta p = C*(U)^{n} \qquad (3)$$

Values for the constant, C, and the exponent, n, can be determined by measurement of pressure drop when the velocity is known, as in a wind tunnel. For example, figure 2 gives wind tunnel data and curve fits for the pressure drops across an isolated Windstar air conditioning condenser, and an isolated radiator. (Normally, the condenser is located immediately forward of the radiator. The data were supplied by Barry Blumel of Ford Motor Company.) For the condenser, the solid curve is the fit with C=0.0607, and n=1.621, and for the radiator, the solid curve is the fit with C=0.0837 and n=1.621.

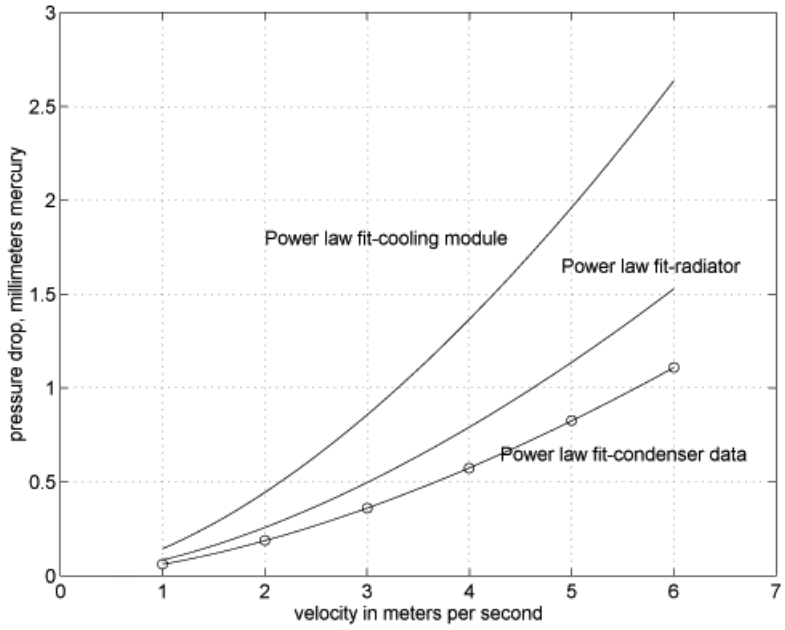

Figure 2. Pressure drop data and fitted power law.

In practice the condenser and radiator form a module, the cooling module. The condenser pressure drop and the radiator pressure drop can be combined to form the cooling module pressure drop. For the Windstar in question, the cooling module pressure drop is given by the expression:

$$\Delta p = (.1444)*(U)^{1.621} \qquad (4)$$

Once C and n are known, the calibration expression can be inverted to yield velocity

given values of pressure drop. Note that this expression will also apply locally across the module in its proper operating configuration.

Cooling module air flow measurements are normally conducted with the full scale vehicle situated in a wind tunnel. The engine is usually not running, and power to operate the cooling fans is supplied by an outside source. (Cooling fans augment the radiator air flow, and since they are downstream from the radiator they do not affect the local relationship between pressure drop and velocity.) The pressure drops to be measured are on the order of several millimeters of mercury, or several inches of water, at sixty miles per hour. Manometers or more sensitive pressure measuring transducers may be used. It is common procedure to average the pressure drop at the measurement points—usually 40 or more—to create an average pressure drop for the module, and then to apply the above relationship to determine an average flow velocity. Multiplying velocity by the cooling module area gives the desired cooling module air volume flow. In a sense, this is the lowest order approximation. Actually, there are many obstructions ahead of the module, such as grill pieces and the front bumper, which make the flow *non-uniform* at the module face. Nothing in principle would keep one from applying the calibration results *locally* at the cooling module face, and to then perform an appropriate local, area-weighted integration to obtain what would be expected to be a more accurate approximation. This procedure is not usually carried out, but see Hucho (1987).

2. The present measurement procedure

Since no sufficiently large wind tunnel is available, the present tests are carried out in the field. This complicates matters in several respects. All instrumentation must be carried along, and powered on-board by means of an inverted 110 volt AC supply. The engine is now operating, and expression (2) relating stagnation pressure and total pressure must be reexamined in the light of possible air density variations across the radiator due to air temperature changes. In addition, the altitude at the location of the test track (HPCC) is 2040 feet above sea level, and the calibration result, expression (4) —to be useful—must be corrected for differences in air density which result from differences in pressure and temperature. Finally, there are uncertainties which result from the relative motions between the two vehicles, and from the presence of winds. These unavoidable effects are minimized by retaining drivers with considerable skill and determination to keep relative motion to a minimum (Patrick Hong and Bogdan Marcu), and by conducting the tests as close to a “no wind” condition as possible.

a. Driving protocols

Cooling module air flow determinations are made for the six vehicle spacings: s = 0.22, 0.28, 0.38, 0.62, 0.88, and 1.0 vehicle lengths, and for three forward speeds 50, 60 & 70 mph (22.4, 26.8, & 31.3 m/s). Measurements are also recorded for the single vehicle in isolation, which may be regarded as the seventh spacing, $s = \infty$. Spacings are provided by cables of fixed length connecting the two vehicles. Figure 3 is a photograph of the two vehicles on the HPCC track. In this case the spacing is 0.22. The forward vehicle is

the tow vehicle. The trail vehicle (our Windstar) is the instrumented vehicle.

Figure 3. Windstar vans on test track at HPCC.

The spacings given above represent bumper-to-bumper spacing. The numbers are accurate to within 1-2 cm. During close following, a certain relative lateral motion is inevitable. These motions can arise as a result of bumps and dips in the roadbed, or from slight wind gusts. There is also a built-in aerodynamic unsteadiness in the van flow itself, which provides a lateral forcing. This is particularly evident and most critical at the shorter spacings. The maximum lateral relative displacements, as estimated from observation marks on the vehicles, are approximately ±15 cm (±6 inches).

The Ford Windstar cooling system contains two electrically driven fans. Both fans are switched automatically on when coolant temperature exceeds 102^{o} C and are switched off when coolant cools below 99^{o} C. This uncertainty is inconvenient for our testing. An override switch is installed to provide the two well-defined test conditions: both fans off, or both fans on. For each speed and vehicle separation, data is recorded for these two conditions. In all, a single set of data corresponds to 7x3x2 = 42 separate runs. Data runs consist of repeated circuits at fixed speed on the HPCC oval track while fans-on/fans-off data is recorded. The speed is changed and the process repeated. When all three speed are accomplished, the separation distance is changed.

The data presented here results from two separate trips to HPCC, during the periods May 5-7 and May 20-22. The runs accomplished on May 7 and on May 22 were recorded

under conditions of very light winds. They constitute two complete and independent sets of data, or 84 runs in all. An additional 15 single-vehicle runs are recorded on Los Angeles area freeways under conditions of light wind and no traffic (late night runs). This brings the total usable run count to 99. Since each run requires about 5 minutes to complete (see section e.), the total data acquisition time is approximately 8.5 hours.

In addition to pressure and temperature data acquired at the cooling module of the test van, we take advantage of the ambient conditions monitored by HPCC (at one minute intervals continuously). The exact time for each run is noted in our log, and these times are matched with HPCC records of barometric pressure, temperature, wind speed and wind direction. Barometric pressure and ambient temperature are used in the estimation of air density. The wind speed (and direction) are used to insure wind speed is sufficiently low to be ignored.

b. Relation between stagnation pressure and static pressure differences when density varies slightly

To reiterate, expression (2) demonstrates equality between the stagnation pressure difference, as measured by the Kiel probes, and the desired pressure difference for air of uniform density. When the engine is running, a temperature difference exists across the cooling module, and the air density is no longer constant. However if the density difference is small—as it is—an approximate expression for the difference can be obtained from (2) to be:

$$p_{o1} - p_{o2} \approx p_1 - p_2 + (1/2)*\rho_1*U_1^2*[\Delta T/T_1] \qquad (5)$$

where ΔT is the air temperature difference across the module. The second term on the right hand side can be regarded as an error term. From measured temperature differences across the module, we determine that the error term is typically of the order of several Pascals, or equivalently, O(0.010) mm Hg. This error is comparable to the least count error (1 bit) in our digitizing scheme, and is small enough to neglect.

c. Extending the calibration curve to accommodate altitude change

A more general expression than equation (4), and one which must be correct on dimensional grounds is:

$$\Delta p = (1/2)*\rho*(U)^2*\text{function}(Re) \qquad (6)$$

where Re is shorthand for Reynolds number, $Re = \rho Ud/\mu$. Here d is a scale for radiator fin spacing, and μ is the viscosity of air. Expression (6) and expression (4) can be made consistent only by postulating

$$\Delta p = K_o*(1/2)*\rho*(U)^2*(\rho Ud/\mu)^{-.379} \qquad (7)$$

where K_o is a non-dimensional constant determined to be 1.535. An additional bit of

manipulation results in an expression for the local velocity at some point on the cooling module, given the pressure difference at that point.

$$(U/U_\infty)^{1.621} = [(\Delta p/q_\infty)*(Re_\infty)^{.379}]/[K_o*(T_\infty/T_{av})^{.356}] \qquad (8)$$

The subscript ∞ stands for ambient atmospheric conditions at the vehicle speed, and q_∞ is shorthand for $q_\infty = (1/2)\rho_\infty(U_\infty)^2$. The quantity T_{av} is the average temperature at the module. We arrive at this number by averaging local temperatures just in-front and just behind the cooling module. The entire right hand side is known at the pressure measurement points, and provides consistent estimates for local velocities at the cooling module for any ambient pressure and temperature.

d. Placement of probes

Pressures are measured at 16 points fore-and-aft of the cooling module (a total of 32 pressures). In figure 4, the 16 locations are superimposed on a close-up of the front of the Windstar. Pressure measurement points lie at the centers of the 16 numbered rectangles. The probe positions are chosen to represent the variety of conditions, produced by bumper and grill obstructions, at the face of the cooling module. For example, positions 1-4, 8-10, 13-16 represent areas of relatively unobstructed flow, while 5-7, 11, 12 are greatly obstructed areas.

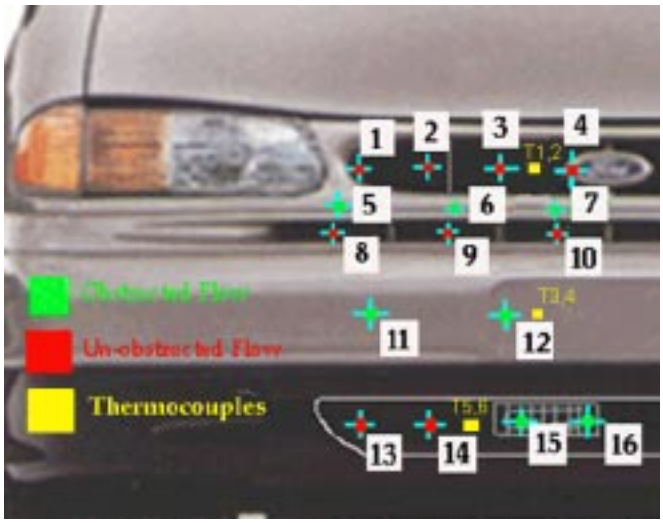

Figure 4. Kiel probe and thermocouple locations for cooling flow measurements.

The rectangular area surrounding each measurement point is taken to be the area of influence. In our local integration scheme, volume flow is computed by multiplying the local velocity estimate by the surrounding area and summing over all areas. This seems to us a more reasonable approach than simply dividing the module face into equal area contributions. The precise locations of each of the Kiel probe pairs is shown in figure 5. Also shown in figure 5 are the locations of the three thermocouple pairs (six temperatures

in all). These pair positions are again chosen to be representative of various portions of the radiator face taking into account the forward obstructions. Thus, thermocouples 1, 2, 5, 6 are in relatively unobstructed portions of the core, while sensors 3, 4 are situated behind the front bumper obstruction.

Notice that only *half* the module face is instrumented. This would provide complete information in every respect provided the vehicle possesses a vertical plane of symmetry. However, the engine placement and the two fan placements are *not* symmetrical, and that exact airflow measurements cannot be obtained by simply doubling our estimates. We have chosen to present the results for airflow over the instrumented half of the radiator, rather than to include the multiplicative factor of (approximately) two.

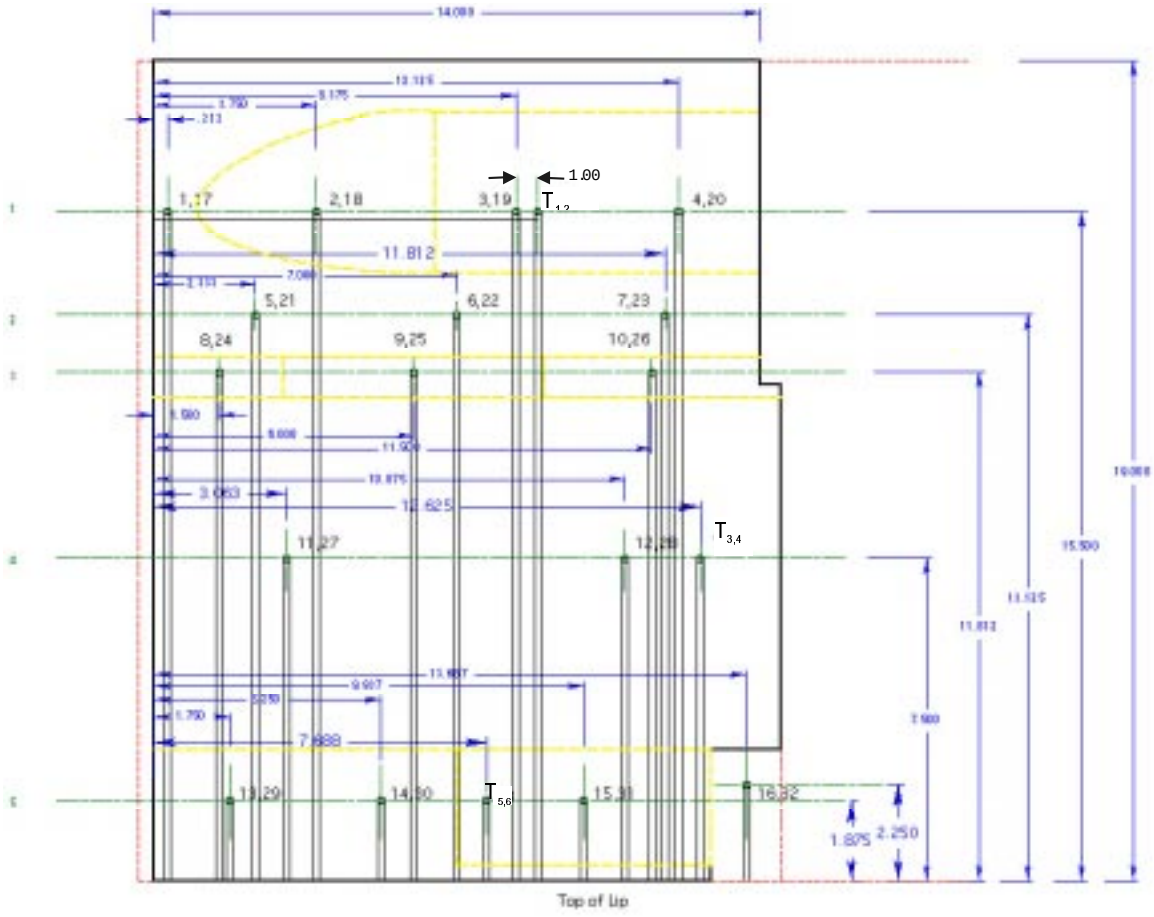

Figure 5. Precise probe locations.

However, the most important measurement quantity is the *ratio* of cooling flow in close-following to cooling flow in isolation. Since close-following does not introduce additional asymmetry, the *ratio* is determined correctly.

e. Recording instrumentation, data acquisition

A schematic of the pressure instrumentation mounted in the Windstar van is shown in figure 6. Pressure tubes from the Kiel probes are routed to a Validyne sensor and to an MKS Baratron sensor through a Scanivalve. The Scanivalve distributes each pressure sequentially to the pressure measuring instruments. Since pressure sensors are differential gages, an appropriate pressure must be available for use as a reference. We are only interested in differences in pressure across the cooling module; the reference pressure (for each pair of pressures in Δp) will cancel out by subtraction and need not be known. However, it must remain constant—at least over the time required to make the measurement of each pair of pressures. The Validyne sensor is referenced to the stagnation pressure recovered from a boom mounted above the roof of the van. The boom stagnation pressure (under conditions of no wind) is the sum of the barometric pressure and the dynamic pressure, q_∞. The Baratron sensor is referenced to an unknown but constant pressure in a container carried in the van. There is redundancy in the use of two pressure sensors. Both pressure sensors are employed independently, and the resulting estimates of pressure (or velocity) are treated as independent samples to be averaged. The pressure sensors are inherently linear devices, and both give outputs of ±5 volts DC for a full scale pressure difference of ±1332 Pa (±10 mm Hg). By way of comparison, the dynamic pressure at a speed of 27 m/s (60 mph) is the order of 600 Pa, and a typical pressure difference across the cooling module is of the order of 400-500 Pa (3-4 mm Hg)

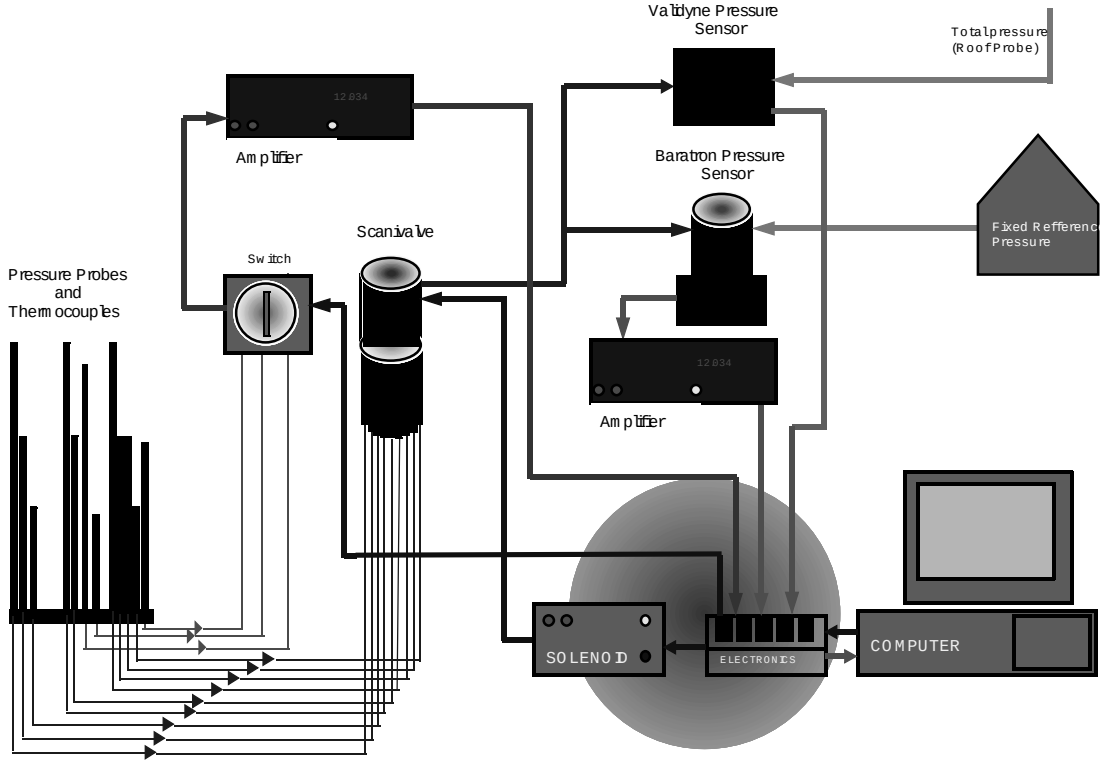

Figure 6. Schematic of pressure instrumentation.

Thermocouple beads and the necessary amplification are purchased from Omega®. The thermocouple bead temperatures are referenced to the temperature of the thermal strip on the amplifier. The output voltage is ±3 volts for full scale temperature difference of ±100°C.

Vehicle speed is measured by means of a Datron optical sensor mounted on a bracket near the front bumper. The Datron provides an analog estimate of forward speed by performing a real time cross-correlation of the signals from two sensors receiving reflected illumination from two small patches of the roadbed displaced in the direction of travel. The cross correlation of the two signals peaks at a time interval which is linearly dependent upon forward speed. The sensitivity of the Datron is 90mV per meter per second (40mV per mile per hour).

The heart of the data acquisition system is a Pentium-75 Laptop utilizing the National Instruments DAQ-700A/D PCMCIA interface card under the operation of LabView software. The card is capable of 12 bit digitization (2048 bits = ±5volt full scale output), giving a least-count pressure accuracy of ±0.65 Pa (±0.005 mm Hg) for either of the pressure transducers, and a least count temperature accuracy of about ±0.08 °C. Least-count speed accuracy is approximately ±0.03 m/s (±0.06 mph).

A typical run corresponds to a fixed speed and a fixed vehicle separation. LabView acquires data sequentially from each of the two pressure sensors and from the Datron for a period of eight seconds (a total of 1024 digitizations per channel). At the completion of an 8-second sequence, the Scanivalve is stepped under computer control until all thirty two pressures are recorded. The six cooling module temperatures are then recorded, and all 8-second records of speed, pressure, and temperature are stored as a mean value and a standard deviation. Each run requires approximately five minutes to complete.

f. Putting it together

To produce an estimate of air flow for the cooling module, the following procedure is employed for each run. The right hand side of expression (8) is first determined. the quantities Δp and T_{av} are know at many points across the radiator, as are the vehicle speed and all ambient quantities appearing with the subscript ∞. The data points for identical runs on May 7 and May 22 are averaged to produce more reliable values. Two integration schemes are then considered. In the first, as is common practice in the industry, the pressure differences at various points over the cooling module face are averaged to produce a single average pressure drop for the module. The average velocity corresponding to this pressure drop is determined from expression (8). Multiplying average velocity by the area of the cooling module (half the module in our case) gives an estimate for the total volume flow. The second scheme is to determine a local velocity at the module face corresponding to each pressure measurement. These local velocities are weighted by the surrounding area—as discussed in section **d**—to produce a volume flow estimate. In practice, these two schemes give almost identical results.

Cooling volume flow estimates require an estimate of accuracy. Several individual values are not sufficient to make an estimate of the standard deviation of the measurements. However, for the single vehicle in isolation, we have 8-12 identical runs at each speed. These runs are used to estimate a standard deviation. We believe this standard deviation is also a reliable indication of the accuracy for the volume flow estimates during close-following.

Matlab is utilized extensively for the data processing. A complete listing of the programs and the data is available upon request.

III. Cooling Module Volume Flow Results

1. Cooling flow for one vehicle in isolation

We first present the single Windstar van air flow results in figure 7. Volume flow is measured in cubic meters per second, and speed is given in meters per second and miles per hour. Two sets of data are shown corresponding to the two operating conditions: both cooling fans on (w/fans), or both cooling fans off (n/fans). The circles represent averages of 7-11 separate runs for the case of n/fans, and three separate runs for the case w/fans. The plus symbols represent ±one standard deviation. These volume flows have been obtained by averaging the pressure drop over the face of the cooling module, by determining a single, average velocity using expression (8), and by multiplication by the half area of the radiator (0.1716 m^2). These will be referred to as the radiator-averaged results.

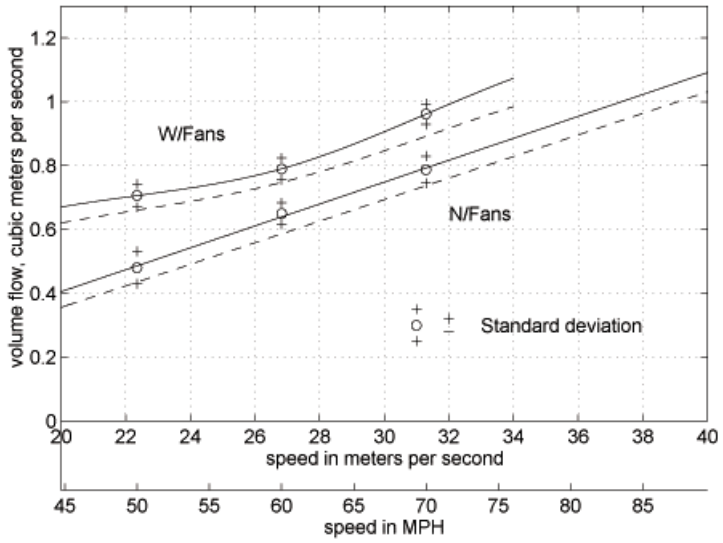

Figure 7. Cooling module volume flows for single van in isolation.

Consider first the case with no cooling fans operating. The solid line is a least squares straight line fit for the three velocities. The means lay very close to this line, and indicate a linear dependence between cooling volume flow and vehicle forward speed. This result can be interpreted by utilizing dimensional arguments. According to the equations of fluid motion, the cooling air velocity must depend only upon forward speed and Reynolds number in the following general form:

$$U_{module} = U_\infty * \text{function}(Re_\infty) \qquad (9)$$

Stated in words, the velocity at the cooling module must depend upon the product of forward speed and an unknown function of the Reynolds number. (Here, the Reynolds number is $Re_\infty = (\rho U H/\mu)_\infty$, where H might be taken as the lateral scale of the vehicle).

Evidently, the dependence upon Reynolds number is slight—as we might anticipate for this high Reynolds number flow—resulting in a linear dependence between cooling velocity, or cooling volume flow, and vehicle forward speed.

The volume flow through the cooling module, Q_{module}, can also be compared to a fictitious flow assuming the module to be exposed to the vehicle speed—as would be the case, for example, if the cooling module were separately placed in a wind tunnel at the speed U_∞. The ratio of these two quantities, Q_{module}/Q_∞, might be termed the capture ratio, and is a measure of the efficiency of the flow system (without augmentation by fans). The capture ratio is approximately 14 % at all three forward speeds. Alternatively, the capture ratio can be thought of as an area ratio—the area far ahead of the van, as a fraction of the module area, which contains all the flow passing through the cooling module.

Cooling air flow is augmented by about 25 % when both cooling fans are operating. The increment in volume flow is almost a constant 0.15 m^3/s at the higher van speeds, but a departure from straight line dependence is evident at lower speeds. This is because the fans operate at a fixed RPM, or fixed tip speed, and their influence becomes progressively more important at the lower forward speeds.

The two dotted lines in figure 7 represent the second method for determining cooling air flow, now utilizing each local pressure difference to derive a *local velocity* estimate and weighting these estimates by *local areas* to determine volume flow. These results, termed local area integration, are uniformly lower by about 5 % of the largest values. We have no ready explanation for the difference. One would expect the local area integration to be the more accurate estimate, since it accounts properly for local variations in flow velocity. Lacking any additional information, our best estimate would be the mean of the two curves.

Since only half the module was instrumented, the values of volume flow given represent flow through half the cooling module. One is tempted to double these values to obtain volume flow for the entire module, but there is a small uncertainty in doing so because the fan housings and the engine are not symmetrically placed behind the radiator.

2. Cooling flow for two close-following vans

The most significant results are displayed in figure 8 and figure 9. Figure 8 plots cooling module volume flow as a function of the separation between the two vehicles, expressed as a per cent of the bumper-to-bumper vehicle length (4.88 meters = 16.0 feet), for fans-on and fans-off operation, and for three forward speeds. Figure 9 expresses these same results, now as a nondimensional volume flow ratio: (volume flow in close-following)/(volume flow in isolation). The two presentations complement one another, although we believe the *volume flow ratio* is our most reliable experimental result. The ratio does not suffer from the uncertainty caused by slight lack of symmetry in the engine compartment mentioned in the previous paragraph. This is because the flow estimates

with vehicle in isolation and with vehicle in close-following have the identical asymmetry, which cancels out when the ratio is formed.

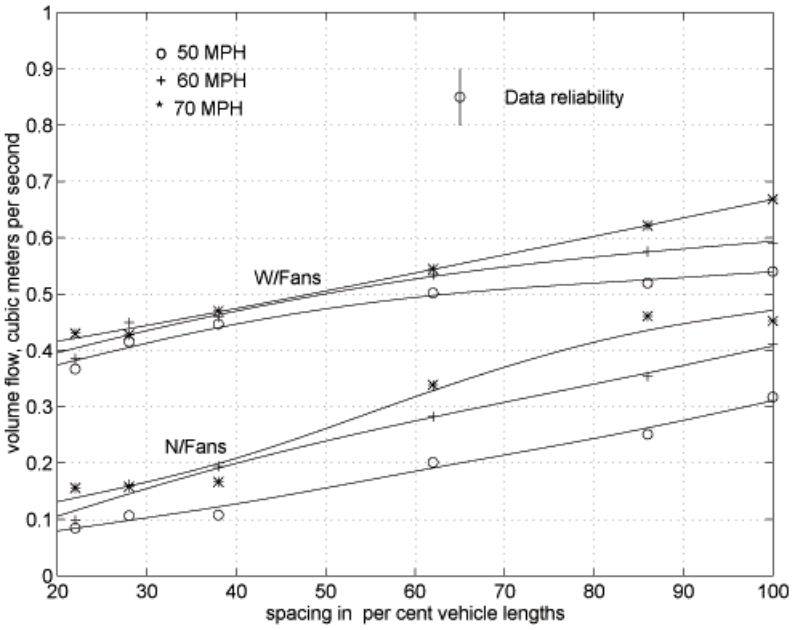

Figure 8. Cooling air flow for two close-following vehicles.

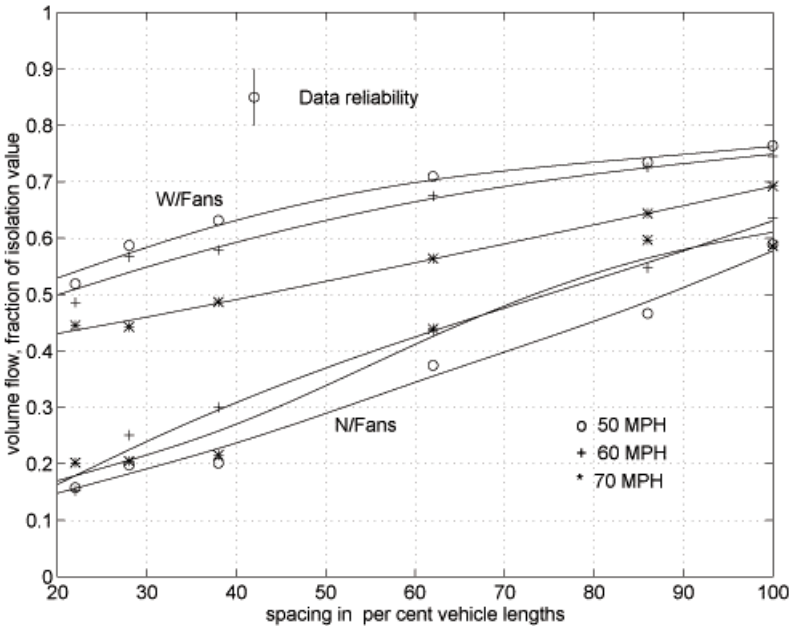

Figure 9. Cooling air flow ratio for two close-following vehicles.

The curves in figures 8 and 9 are smoothing cubic splines chosen to lie within the bounds of the reliability estimated from the standard deviation of the single vehicle runs.

Consider first the absolute volume flow estimates in figure 8, and observe the trends. (Again, as in the previous section, these volume flows refer to half the cooling module, and should be doubled for an estimate of total flow.) At short spacings 0.22, 0.28, 0.38 lengths, the volume flow is relatively insensitive to spacing changes or to vehicle speed. Volume flows are approximately 0.12 m^3/s with no fans, and more than a factor of three times larger with fans operating. This enormous difference is a reflection of the low speeds existing within the gap between vehicles at relatively short spacings.

As spacing increases beyond one-half vehicle length, a stronger dependence between volume flow and forward speed becomes clear, while the augmentation produced by the cooling fans has been reduced to about fifty per cent. Note that this augmentation is still considerably larger than the augmentation for the vehicle in isolation (about twenty-five per cent).

Consider now the same results interpreted as ratios, first with no fans operating. At short spacings, the volume flow is about twenty per cent of the value for vehicle alone, and this value is not strongly dependent upon vehicle speed or upon spacing. This is a very substantial decrease in cooling flow. It is safe to say the vehicle could not operate for long in such a condition without overheating. As spacing increases, the volume flow rises to about sixty per cent of the vehicle alone value, and still represents a substantial diminution. This again is a reflection of the sheltering effect of the forward vehicle. For the "no fans" conditions, there is little dependence of the ratio upon vehicle speed for any of the spacings studied.

When both fans are operating, the cooling volume flow is approximately half of the vehicle alone result at the shortest spacing, and increases to about seventy per cent at a spacing of one vehicle length. These results show a definite dependence upon speed—the lower the vehicle speed, the more efficient the cooling fans are in providing some additional volume flow while in a close-following situation.

3. Meeting cooling flow requirements

The cooling volume flow measurements presented here are specific to a certain vehicle. The results can be expected to be different for a different vehicle, one, say, possessing a differently designed front end shape, or a vehicle having a different radiator housing or radiator area, or different fan performance—to name just a few possible dissimilarities. However to the extent that all vehicles of similar size and horsepower will have similar cooling flow requirements, we do believe the results are representative of a number of modern vehicles.

The cooling volume flow *ratio* can be expected to be much less affected by specific geometries than are the absolute volume flow values. Vehicle bumper geometry in the vicinity of the cooling flow inlets, and the internal duct geometry, both have a pronounced influence upon the cooling flow for the vehicle in isolation, but these

localized differences probably do not alter the overall external flow field, and—to lowest order—will not affect the volume flow *ratio*. Much information on the generality of these results could be obtained in the future by performing similar measurements on vehicles of several widely different shapes.

Qualitatively, the cooling flow must carry away a quantity of heat energy which is a substantial fraction of the total useful engine power output. This useful power is needed to overcome rolling resistance and aerodynamic drag, to accelerate the vehicle, to lift the vehicle in hilly terrain, and to operate auxiliary equipment such as air conditioning. From the known relationship between useful power consumed and heat production, one can in principle determine the minimum required cooling volume flow. For steady, non-accelerated travel of most interest here, the minimum required volume flow for a particular vehicle will depend primarily upon vehicle speed, climbing angle (road slope), and ambient temperature. For example, figure 10 sketches qualitatively the *required minimum* cooling flow as a function of vehicle speed for a level road and fixed ambient temperature. Also shown are the two curves (as in figure 7) corresponding to the *available* cooling flow. Where available cooling flow exceeds required flow, there is (positive) cooling margin.

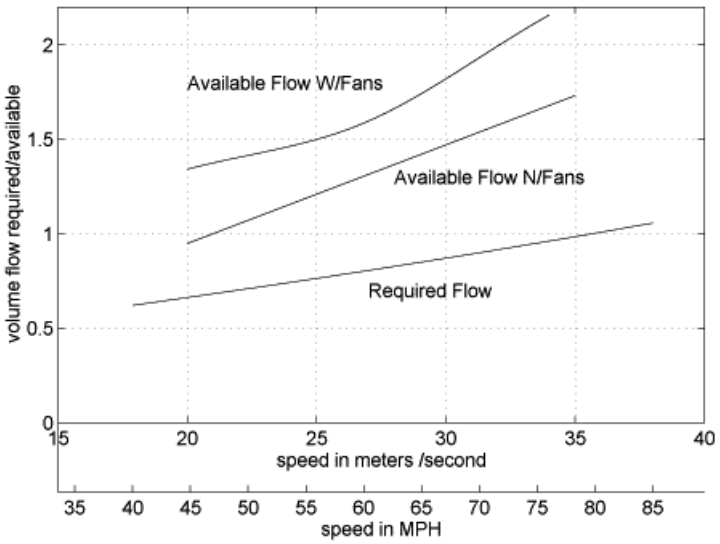

Figure 10. Sketch illustrating cooling margin.

For a modern automobile, there is positive cooling margin for virtually all operating conditions likely to be encountered. However, figure 9 illustrates that available cooling flow is diminished by a factor of approximately 0.5 in a close-following situation—for the case of both fans operating. When the vehicle in isolation is operating near the limit of cooling power, as for example might occur during a hill climb on a hot day, there would likely be insufficient cooling flow for close-following operation under identical ambient conditions. Thus, the operating envelope of the vehicle is altered for close-following, and it almost certainly would be diminished in size. We will attempt to estimate what these changes might be.

a. Derivation of the required cooling flow

Let the heat flux for removal by the cooling module be **Q**. Let the useful engine power expenditure be **P**. There exists an empirical relation of the form:

$$\mathbf{Q} = \mathbf{P}^{*}\text{function}(\mathbf{P}/\mathbf{P}_{max}) \tag{10}$$

where $\mathbf{P}_{max}$ is the maximum engine power. The function of **P** is sometimes expressed as follows.

$$\text{function}(\mathbf{P}/\mathbf{P}_{max}) = C^{*}(\mathbf{P}/\mathbf{P}_{max})^{n} \text{ , with } n \approx -1/2 \tag{11}$$

The heat flux can also be expressed as the product of a mass flow rate, W, and the relevant temperature difference. For the cooling module this is:

$$\mathbf{Q} = W^{*}(T_f - T_\infty)^{*}c_p \tag{12}$$

where T_f is the final temperature of the air on the engine side of the cooling module, and T_∞ is the upstream, or ambient air temperature. The constant c_p is the specific heat of air. Forming the ratio of heat flux in close-following compared to heat flux for the isolated vehicle—and noting that the power expended during close-following is reduced because the drag is less—gives an expression for the ratio of required flow rates.

$$W_p/W_i = [(T_{fi} - T_\infty)/(T_{fp} - T_\infty)]^{*}[1 - 0.25^{*}(\rho S U_\infty^{3} \Delta C_D)/(\eta_{DT}^{*}\mathbf{P}_i)] \tag{13}$$

The area, S, is cross sectional area of the vehicle (in the forward direction), and ΔC_D is the change in drag coefficient associated with close-following at a given spacing. The additional subscripts p and i stand for platoon (close-following) and isolated operation, respectively, and use is made of the fact that the second quantity in the last bracket is small compared to unity. In words, this relationship says that the ratio of required flow rate for close-following compared to the required flow rate for operation in isolation depends upon two multiplicative factors. The first factor is a ratio of temperature differences across the cooling module for isolated and close-following operation. In a sense, the temperature difference $(T_f - T_\infty)$ is a measure of the effectiveness of the cooling system at a given operating point. When the temperature difference is small, there is more than sufficient cooling flow to carry away the heat produced. A large temperature difference indicates that the cooling system is working near its limit to transfer heat. The maximum incoming liquid temperature in the radiator is limited to about 120°C. Since the air temperature leaving the cooling module must necessarily be less than the incoming liquid temperature, T_f is limited to a temperature of approximately 90-100°C. The second factor in determining the ratio of required cooling flows represents the relative decrease in power expenditure due to the diminished drag in close-following operation. It is a number less than unity. The power expenditure for the vehicle in isolation, $\mathbf{P}_i$, can be estimated at any desired operating point. The quantity η_{DT} is the

drive train efficiency—usually taken to be approximately 0.9. Since the decrease in drag upon entering the platoon is also known from our previous measurements (e.g., Zabat et al. (1995), Hong et al. (1998), Browand et al. (1997)), the second term is known.

The procedure for determining the availability of sufficient cooling flow is to compare expression (13) for the ratio of *required* cooling flows with the measured ratio of cooling flows *available* in figure 9. If the *available* flow is greater than the *required* flow, then close-following is possible with the existing vehicle. If the *required* flow exceeds *available* flow, some modification would be required to improve cooling performance for close-following operation. Since we are looking for the *minimum required* cooling flow during close-following, we can set T_{fp} to its largest possible value, say $T_{fp} = 90°C$. For a given vehicle operating point, $\mathbf{P}_i$, and prescribed ambient temperature, T_∞, the only uncertainty remaining in expression (13) is the temperature, $T_{fi,}$ or $(T_{fi} - T_\infty)$. The value of T_{fi} or $(T_{fi} - T_\infty)$ for a particular speed and climb angle (road slope) is specific to a particular vehicle, and we would need such information to proceed. In the absence of such detailed information at present, we will perform several sample calculations to illustrate the procedure.

b. Example calculations

We will consider two operating points which would be typical for the Windstar van. The first point corresponds to steady operation on a level road on a moderately warm day, $T_\infty = 32°C$. For this case, we have recorded temperature data for the Windstar giving $T_{fi} \approx 39°C$ with fans-on and $T_{fi} \approx 46°C$ with fans-off. The expression for power is of the form:

$$\mathbf{P}_i = C_0 + [(A_0 + Mg*Sin\theta)*U_\infty + A_1*(U_\infty)^2 + (\rho/2)*C_D*S*(U_\infty)^3]/\ \eta_{DT} \qquad (14)$$

A_0 and A_1 are rolling resistance terms, $\sin\theta$ is the road slope, and C_0 is the power expended by auxiliary equipment. Take $C_0 = 4476$ W, $A_0 = 191$ N, $Mg = 17{,}800$ N, $A_1 = 3$ N/m/s, $C_D = 0.35$, $S = 2.8$ m^2, $\rho = 1.16$ Kg/m^3, $\eta_{DT} = 0.9$, as representative of the Windstar van for the three speeds $U_\infty = [22.6, 26.8, 31.3]$ m/s, (corresponding to [50 60 70] mph).

Figure 11 illustrates the results of the calculation graphically. The curves in figure 9 are reproduced corresponding to flow *available* with and without fans for the separations between 0.2 and 1.0 vehicle lengths. Superimposed on this plot are the two results of the calculation, equation (13), for the conditions with fans and without fans. These correspond to estimates of flow *required.* The required cooling flows are virtually independent of speed (the three curves are nearly superimposed), and there is negligible

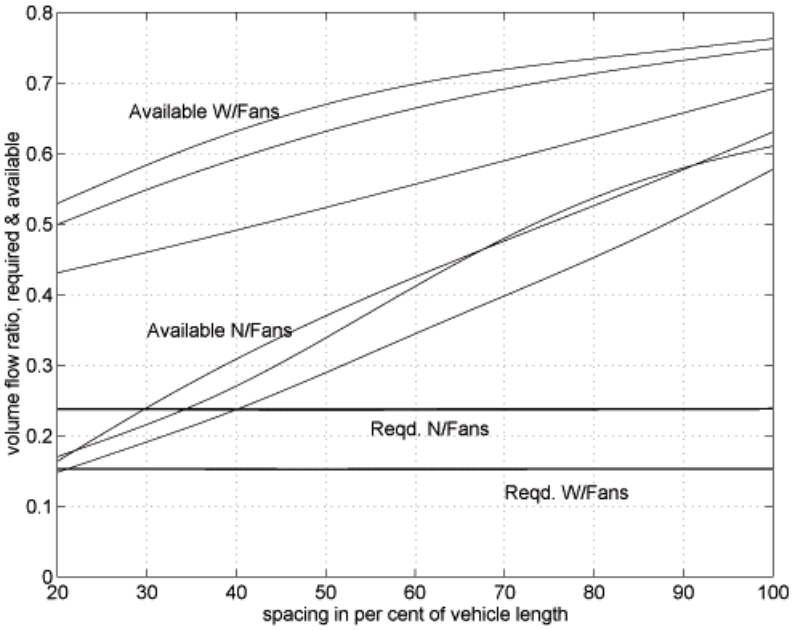

Figure 11. Example of cooling margin for close-following vans on a warm day.

dependence upon the particular value of separation. The reason is that although there is a drag reduction of .25—.35 for the trail vehicle in a two-vehicle platoon, the drag reduction is not a strong function of separation. That is, the second term in expression (13), containing the variation in drag coefficient and speed, is in this case nearly constant. The results indicate a large cooling margin at all separations for operation with fans. There would be insufficient cooling margin at the shorter spacings—0.2-0.4 vehicle lengths—to operate without cooling fans.

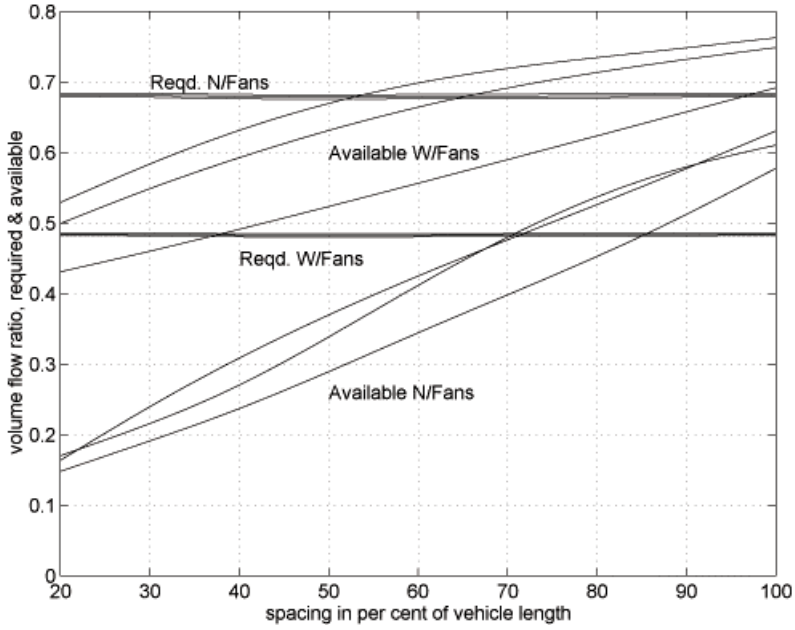

Figure 12. Cooling margin under more extreme conditions.

A second, more critical condition supposes climbing on a three degree slope on a slightly warmer day, T_{amb} = 35°C. Representative values for radiator outlet temperatures are $T_{fi} \approx$ 73°C for fans-off and 62°C for fans-on. Figure 12 gives the estimated cooling flow requirements, and the cooling flows available for two close-following vehicles. With fans-off, there is insufficient cooling flow available to close-follow at any separation for any of the three speeds tested. It is also seen that close-following would not be possible even with fans-on at the highest speed and shortest separations. Operating under these conditions—or under more severe conditions—would require modification to the existing cooling system.

c. Extending present results to longer platoons

It is not likely that cooling flow will be measured for platoons of more than two vehicles. Estimates such as those presented in figures 11 and 12 might be made for longer platoons by simply assuming the same diminished cooling flow available to each of the vehicles in the platoon. Strictly, this is not correct. The nearest forward vehicle undoubtedly has the most influence upon the flow over the forward portion of the trailing vehicle. However, the effect of several forward vehicles must be to generate a larger momentum deficit and thus a larger layer of slow moving air surrounding the platoon (as viewed in the coordinate system moving with the vehicles). In a longer platoon, the flow available to the radiator would thus probably be somewhat diminished from the result presented in figure 9. There are also additional drag savings for vehicles in longer platoons, and these would reduce the power required and the required cooling flow (by decreasing the second factor in expression (13)).

Acknowledgments

Support for this research program was provided by the California Department of Transportation, under a grant administered by California PATH, University of California at Berkeley.

We also gratefully acknowledge the able technical assistance of Thane DeWitt, Mark Trojanowski, and Aaron Tucker.

References

1. Browand, F., Zabat, M., Tokumaru, P., "Aerodynamic benefits from close-following", *Automated Highway Systems*, ed. P. Ioannou, Plenum Press, (1997), Chapter 12.

2. Hong, P., Marcu, B., Browand, F., Tucker, A., "Drag forces experienced by two full-scale vehicles at close spacing. *Society of Automotive Engineers*, Paper No. 98B-175 (1998).

3. Hucho, W-H., *Aerodynamics of Road Vehicles*, Butterworth-Heineman, (1987), Chapter 9.

4. Kanaris, A., Ioannou, P., Ho, F.-S., "Spacing and capacity evaluations for different AHS concepts", *Automated Highway Systems*, ed. P. Ioannou, Plenum Press, (1997), Chapter 8.

5. Zabat, M., Stabile, N., Frascaroli, S., Browand, F., "Drag forces experienced by 2,3, & 4 vehicle platoons at close spacings", *SAE Paper No. 950632*, (1995).